Check for updates

Received: 14 March 2024 | Revised: 16 August 2024 | Accepted: 24 October 2024

DOI: 10.1111/ijag.16695

INTERNATIONAL JOURNAL OF Applied Glass SCIENCE

SPECIAL ISSUE ARTICLE

Flame-impingement-induced superhydrophilicity of soda-lime-silica glass surface

Barsheek Roy* | **Anne Schmidt** | **Andreas Rosin** | **Thorsten Gerdes**

Keylab Glass Technology, University of Bayreuth, Department of Engineering Science, Bayreuth, Germany

Correspondence
Barsheek Roy
Email: roy.phdadm@gmail.com

Funding information
Bayerisches Staatsministerium für Umwelt und Verbraucherschutz, Grant/Award Number: BAF0150Fo-74094; University of Bayreuth

Abstract

The importance of superhydrophilicity of glass surfaces lies in their self-cleaning abilities. The need for antifogging characteristics of soda-lime-silica (SLS-) based window glasses requires feasible solutions. Superhydrophilicity is generally achieved by textured surfaces with suitable features or any chemical modification including thin films. Fabrication of textured surfaces usually involves sophisticated facilities that are often expensive. This paper reveals a novel approach to achieving superhydrophilic SLS surfaces by flame-impingement. The chemical energy of methane gas was converted into thermal energy by a flame torch to reach temperatures just above the softening point of SLS glass. The glass surface was exposed to the flame at a distance of around 100 mm for 10 s. The surface was transformed into a superhydrophilic state with a static contact angle of nearly zero after the treatment. This property was remarkably retained on exposure of the surface to the ambient atmosphere for 3 years of aging. The subsurface structural modifications accountable for the alteration in wetting behavior by the influence of flame-impingement were investigated. High-resolution X-ray photoelectron spectroscopy of the O1s spectral line evidenced the repolymerization of vicinal silanols into bridging oxygens (BOs), accompanied by the loss of hydrous species ($SiOH/H_2O$) in the near-surface region. The repolymerized BOs acted as adsorption sites of water molecules to promote superhydrophilicity. Atomic force microscopy exhibited the conversion of an open silica tetrahedral network with nonbridging oxygens into closed rings. The high surface energy of the residual surface nanostructure at the solid/vapor interface was accountable for the superhydrophilicity.

KEYWORDS
flame-impingement, silicate network connectivity, soda-lime-silica glass, superhydrophilicity, surface

*Roy Barsheek was selected as an ACerS Rising Star.

This is an open access article under the terms of the Creative Commons Attribution License, which permits use, distribution and reproduction in any medium, provided the original work is properly cited.
© 2024 The Author(s). *International Journal of Applied Glass Science* published by American Ceramics Society and Wiley Periodicals LLC.

1 | INTRODUCTION

Soda-lime-silica (SLS) glass serves a wide spectrum of societal materialization—ranging from window glasses to container bottles. However, the intrinsic brittle characteristic[1] continues to act as a potential barrier to reduce its broader scope of applicability. One of the major reasons is attributed to the inevitable presence of surface flaws that act as stress concentrators—leading to failure strengths, several orders of magnitude lower than the theoretical counterpart.[2,3] The compensation of the difference in magnitude necessitates a thorough perception of the surface structural chemistry that governs the overall performance of the material in terms of mechanical properties, chemical durability, and corrosion resistance.

The glass surface acts as an interface between the external environment and the bulk of the silicate network. It is in constant interaction with the ambient atmosphere to form silanol groups linked to the adsorbed water molecules. The current state of knowledge of the influence on surface structural characteristics caused by the interaction of the near-surface region of SLS glass is limited, with extended emphasis on aqueous corrosion mechanisms forming a surface passivating layer that governs the chemical durability.[4–7] This work is aimed at investigating the modification of the surface structure caused by flame polishing,[8,9] which is a common industrial practice to obtain a relatively smooth glass surface with a homogenous morphology. The technique of flame spraying is commonly used for the application of coatings on glass surfaces.[10] In this work, the chemical energy of methane was converted into thermal energy by a flame torch to reach surface temperatures above the softening point—visually evidenced by the deformed edges of the specimen right after the treatment. The SLS surface was exposed to the flame at a distance of approximately 100 mm from the nozzle for 10 s. The aforementioned process is referred to as "flame-impingement" in this article. The modification of the surface structure caused by flame-impingement was studied in terms of the alteration in silicate network connectivity in the near-surface region as well as the bulk of the glass network. The primary objective was to investigate the surface structural cause of the alteration in wetting characteristics of the glass surface.

The modification of the wettability of SLS glasses to obtain hydrophobic[11,12] and superhydrophobic[13,14] surfaces was a subject of considerable research in the past, catering to tailor-made applications. Similarly, superhydrophilic[15–17] and amphiphilic[18] SLS glasses are of considerable interest for antifogging and self-cleaning applications. The achievement of superhydrophilic thin film metal oxide coatings of ZnO and TiO_2 on glass surfaces by high-temperature annealing has been reported in the past.[19] This research discovered an approach to achieving superhydrophilicity of the bare glass surface by flame-impingement with an everlasting effect. It corroborates the finding of a superhydrophilic glass surface induced by heat.[20] The following sections are intended to shed light on the surface structural modifications caused by flame impingement that are accountable for superhydrophilicity.

2 | RESULTS

2.1 | Silicate network connectivity as a function of depth from the glass surface

X-ray photoelectron spectroscopy (XPS) is a surface-sensitive technique that can be effectively used to study the local bonding environment of oxygen atoms on glass surfaces. The spectral fit of the O1s curve reveals the individual contributions of bridging oxygens (BOs), nonbridging oxygens (NBOs), and hydrous species ($SiOH/H_2O$) corresponding to the difference in binding energies associated with electrostatic interactions.[21–26] A comparative analysis of the O1s spectral line was performed before and after flame-impingement to determine any influence on the surface structural network. The curve-fittings were performed in an unconstrained manner in accordance with our previous studies[24–26] to calculate the areas under the respective peaks. Figure 1 illustrates the comparative O1s spectral representations of untreated and flame-impinged surfaces. The corresponding binding energy, full width at half maxima (FWHM), and normalized integrated peak areas are reported in Table 1. The information depth corresponding to this measurement is confined to a depth of about 5 nm below the glass surface, governed by the inelastic mean free path of the photoelectrons.[27] It is known that the as-manufactured glass surface contains different types of hydroxyl groups like isolated silanols, geminal silanols, vicinal silanols, and adsorbed water in the form of chemisorbed and physisorbed water.[28] Additionally, molecular water may also be trapped in the glass network. The noteworthy difference between the two XPS O1s spectral fits is marked by the absence of hydrous species in the flame-impinged surface accompanied by an increase in the area under the BO peak by nearly 25%. The absence of the $SiOH/H_2O$ peak (blue curve) on the flame-impinged surface was a result of mathematical peak-fitting performed in accordance with our previous studies[24–26,28] to obtain the best fit. The relative increase in the concentration of bridging oxygens and the absence of hydrous species ($SiOH/H_2O$) after

20411294, 2025, 2, Downloaded from https://ceramics.onlinelibrary.wiley.com/doi/10.1111/ijag.16695 by Universitaet Bayreuth, Wiley Online Library on [18/03/2025]. See the Terms and Conditions (https://onlinelibrary.wiley.com/terms-and-conditions) on Wiley Online Library for rules of use; OA articles are governed by the applicable Creative Commons License

TABLE 1 Comparative representation of binding energy, FWHM, and normalized integrated peak area of O1s spectral line of untreated and flame-impinged SLS glass surfaces.

	Binding energy (eV)		FWHM (eV)		% Area	
Peak label	Untreated	Flame-impinged	Untreated	Flame-impinged	Untreated	Flame-impinged
NBO	530.10	530.39	1.62	1.39	20.47	14.52
BO	531.51	532.17	1.35	1.75	61.16	85.48
$SiOH/H_2O$	532.33	–	1.43	–	18.37	–

Abbreviations: BO, bridging oxygens; FWHM, full width at half maxima; NBO, nonbridging oxygens; SLS, soda-lime-silica.

the treatment indicates the repolymerization of vicinal silanols into bridging oxygens, accompanied by the loss of chemisorbed water from the surface. This observation complements the findings of Banerjee et al.[22] pertaining to in situ XPS analysis during sub-T_g (T_g: glass transition temperature) thermal treatment of the SLS glass surface. The BO peak of the flame-impinged surface in Figure 1 is centered on a slightly higher binding energy of 532.17 eV relative to the untreated surface. The NBO peak position is not characterized by any notable shift. The significant increase in the area under the BO peak is reflected by the broader nature of this peak with a slight shift in its position after the treatment. Any other reason to comprehend this shift in the binding energy cannot be explained.

After the first XPS measurement corresponding to the top 5 nm of the glass surface, the subsurface region of the glass network was probed by sequential XPS measurements accompanied by Ar^+ sputtering. The total sputtering duration was 110 min with an estimated etching rate of 1 nm/min.[26] The individual contributions of the oxygen speciations (BO, NBO, and $SiOH/H_2O$) were separately calculated from the O1s spectral fits before and after the flame-impingement process for every data point. The atomic ratios of the different oxygen species to silicon were computed and plotted as a function of Ar^+ sputtering time to analyze the alteration in subsurface silicate network connectivity caused by the treatment. This is illustrated in Figure 2. The total oxygen to silicon atomic ratio O_{total}/Si was close to 3.0 in the near-surface region of the untreated SLS glass.[25,28] It hovered in the range of 3–3.5 after flame-impingement with no significant change. The noteworthy difference is marked by a pronounced increase in $O_{Si-O-Si}$ /Si at the expense of hydrous species in the subsurface region up to a depth of approximately 110 nm below the glass surface. This observation is similar to that of the top 5 nm of the glass surface, as discussed previously. The increase in BO/Si is indicative of silicate network repolymerization. The contribution of $O_{SiOH/H2O}$ was nil after the treatment, as shown in Figure 2B. The loss of hydrous species in association with network repolymerization essentially signifies a condensation reaction. This is characterized by the reaction of two adjacent silanol groups (vicinal silanols) to form bridging oxygen, accompanied by the release of a water molecule shown as follows:

$$Si-OH + Si-OH -> Si-O-Si + H_2O \uparrow$$

The pronounced increase in the atomic ratio of $O_{Si-O-Si}/Si$ to compensate for the decrease in $O_{SiOH/H2O}/Si$ was indicative of network rearrangement that resulted in stronger silicate network connectivity in the subsurface region of the flame-impinged SLS glass. It is to be noted that there was no evidence of volatilization of the modifier cations, sodium, and calcium, after the treatment. The elemental depth profiles of the untreated and flame-impinged surfaces obtained by XPS are reported in the Supporting Information Data. There was no distinguishable influence in the concentrations of the modifier cations up to a depth of about 110 nm below the glass surface (Figure S1). The quantitative distribution of the respective Q^n species in the bulk of the silicate network (wherein "n" represents the number of bridging oxygens linked to a silica tetrahedron) determined by solid-state ^{29}Si magic angle spinning nuclear magnetic resonance (MAS NMR) spectroscopy—succeeds the context of the current discussion.

2.2 | Distribution of Q^n species in the bulk of the silicate network

Solid-state MAS NMR of ^{29}Si was carried out for quantitative analysis of the comparative measure of the alteration of Q^n species in the bulk of the silicate network. The specimens were subjected to spin at a frequency of 10 kHz (with respect to the static magnetic field of 7.05 T) at the magic angle of 54.74° ($3 * \cos^2\theta - 1 = 0$) to average the chemical anisotropy associated with nuclear interactions. This was necessary to prevent peak-broadening to obtain high-resolution spectra, for the subsequent fittings to extract the overlapping peaks,[29] shown in Figure 3. The parameters pertaining to the spectral fits are tabulated in Table 2. The major broad peak corresponding to

20411294, 2025, 2, Downloaded from https://ceramics.onlinelibrary.wiley.com/doi/10.1111/ijag.16695 by Universitaet Bayreuth, Wiley Online Library on [18/03/2025]. See the Terms and Conditions (https://onlinelibrary.wiley.com/terms-and-conditions) on Wiley Online Library for rules of use; OA articles are governed by the applicable Creative Commons License

TABLE 2 Spectral fit parameters of solid-state ^{29}Si MAS NMR of untreated and flame-impinged SLS powder specimens.

	Chemical shift (ppm)		FWHM (ppm)		% Area	
Peak label	Untreated	Flame-impinged	Untreated	Flame-impinged	Untreated	Flame-impinged
Q^3	−91.45	−91.32	13.05	12.48	65.31	60.03
Q^4	−101.03	−100.68	13.89	14.29	34.69	39.97

Abbreviations: FWHM, full width at half maxima; MAS NMR, magic angle spinning nuclear magnetic resonance; SLS, soda-lime-silica.

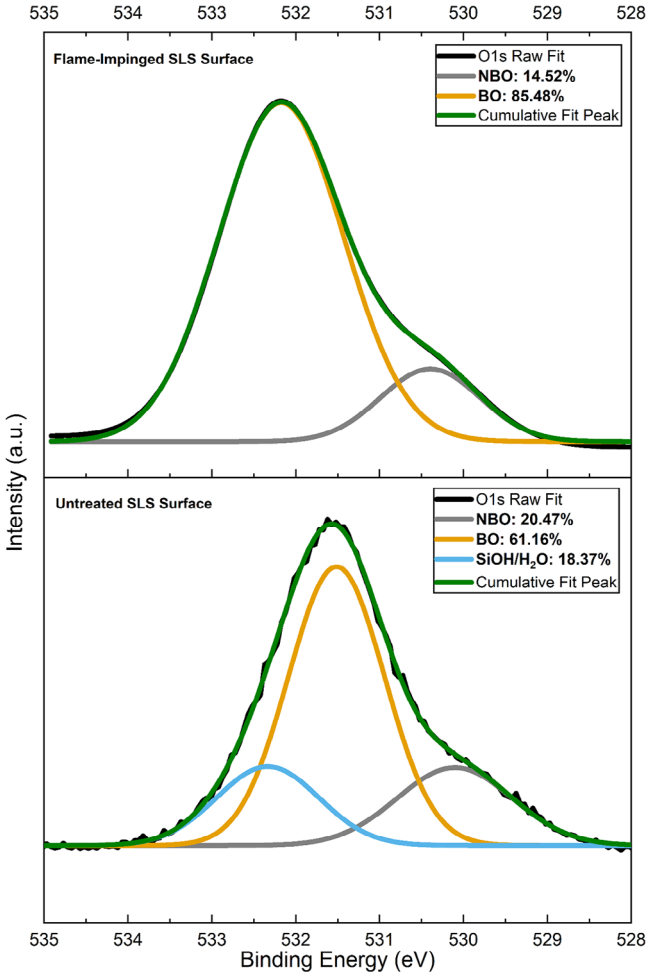

FIGURE 1 Comparative illustration of XPS O1s spectral fits of untreated and flame-impinged SLS surfaces. The respective concentrations of bridging oxygen (Si–O–Si), nonbridging oxygen (Si–O–Na), and hydrous species ($SiOH/H_2O$) obtained by the normalized integrated peak areas are indicated in the legends. The analysis corresponds to the region within a depth of 5 nm from the glass surface. R-square—representative of the goodness of fit, is greater than .99 in both spectral fits. SLS, soda-lime-silica; XPS, X-ray photoelectron spectroscopy.

a chemical shift of around -92 ppm represents Q^3 units, while the shoulder peak around −101 ppm reflects the presence of Q^4 units.[21,30] The nucleus is less shielded with increasing chemical shifts. The normalized integrated peak areas were taken into consideration for quantification of the respective Q^n species. A 5.28%-increment in Q^4 species was observed in the overall silicate network of the flame-impinged SLS specimen at the expense of Q^3 species, indicating enhanced silicate network connectivity. Given the lack of surface sensitivity of NMR, the results in Figure 3 essentially represent an effect of silicate network repolymerization in the volume of the glass network. The effect of flame impingement is more pronounced in the subsurface region causing a significant relative increase in the bridging oxygens by 25% as observed by the XPS results in Figure 1. In comparison, the relative increase in the Q^4 species in the volume of the network is just about 5%. Although the surface, as well as the bulk of the glass network, were affected by flame-impingement, the subsurface region up to a depth of about 110 nm investigated by XPS had a much larger effect of repolymerization than the volume of the glass network.

2.3 | Superhydrophilicity of flame-impinged SLS surface

The surface wettability of SLS glasses may be defined by the nanostructural orientation of the silicate network associated with silanol groups and adsorbed water on the topmost surface. Hydrogen-bonded hydroxyl groups act as natural adsorption sites of physisorbed water. Isolated, free hydroxyl groups at the surface were reportedly found to lower the hydrophilicity.[31]The wetting behavior may also be explained by surface roughness,[32] which, in turn, is arguably governed by the surface structural chemistry at the atomic level. We observed a transition to the superhydrophilic state immediately after the flame-impingement process, represented by a stark reduction in static contact angle from 32° (pristine surface) to nearly zero—as displayed in Figure 4.

The spectroscopic results pertaining to surface structural modifications discussed in the preceding sections—substantiated the evidence of network repolymerization, accompanied by the loss of silanol groups and chemisorbed water effectuated by flame-impingement. The contribution of the loss of silanol groups to enhance the surface hydrophilicity by the virtue of network repolymerization to obtain a closed surface structure of silicate rings

20411294, 2025, 2, Downloaded from https://ceramics.onlinelibrary.wiley.com/doi/10.1111/ijag.16695 by Universitaet Bayreuth, Wiley Online Library on [18/03/2025]. See the Terms and Conditions (https://onlinelibrary.wiley.com/terms-and-conditions) on Wiley Online Library for rules of use; OA articles are governed by the applicable Creative Commons License

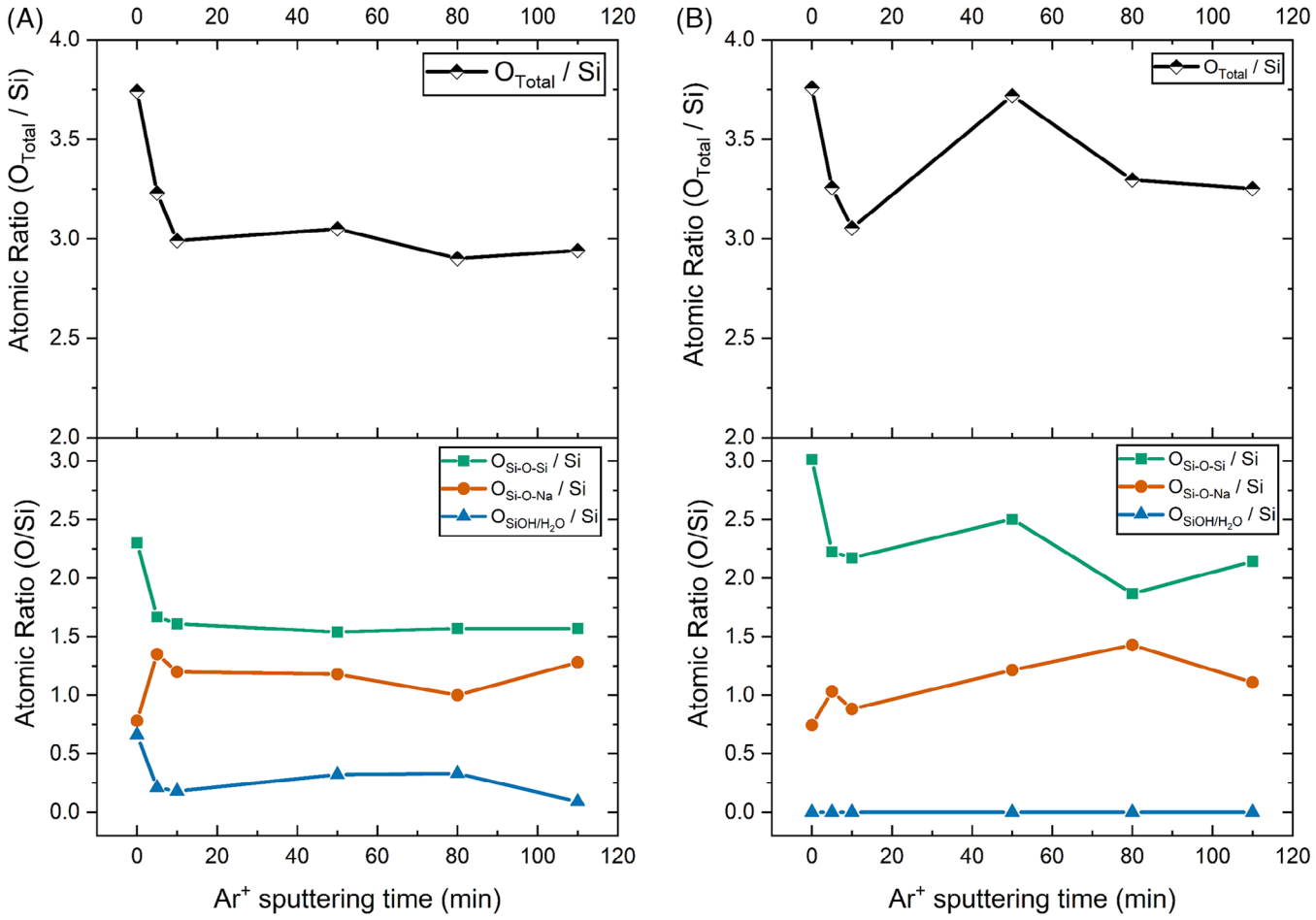

FIGURE 2 Variation of the atomic ratio of individual oxygen speciations to silicon as a function of Ar^+ sputtering time (below); total oxygen to silicon atomic ratio as the sum of individual contributions (above) (A) untreated (B) flame-impinged surface. Connecting lines act as a guideline to the eyes.

increases the surface energy to trigger extreme wettability. The conversion of the open silicate rings into closed forms is portrayed in the AFM images presented in Figure 5.

The flame-impingement mechanism adopted in this study—involves a rapid interaction of the flame with the glass surface to trigger instant evaporation of the surface hydrous species with consequent repolymerization of nonbridging oxygens into closed silicate rings—experimentally evidenced by a substantial increase in the atomic ratio of $O_{Si-O-Si}$/Si. This leaves a residual nanostructure with some closed rings of silica tetrahedral units on the topmost surface. They provide sufficient surface energy at the solid–vapor interface to promote the rapid spreading of the water droplet on the glass surface, causing superhydrophilicity.

The schematic representation of the experimental process with consequent surface structural modifications is illustrated in Figure 6. The repolymerized bridging oxygens indicated on the surface are highly reactive to act as adsorption sites of water molecules for hydrogen bonds.[33] They have a high tendency to form hydrogen bonds with water molecules. This increases the chemical affinity of water on the flame-impinged glass surface to promote superhydrophilicity.

TABLE 3 Static contact angle of the flame-impinged glass surface with respect to water as a function of time.

Contact angle immediately after flame impingement	Contact angle after 1 year	Contact angle after 3 years
~0°	~0°	~0°

It is noteworthy that the superhydrophilicity was retained on exposure of the flame-impinged SLS surface to the ambient atmosphere (~25°C, 60–65% humidity) for 3 years. The contact angle of the surface was monitored after 1 and 3 years of treatment to discover the retention of the superhydrophilicity throughout this period as summarized in Table 3.

20411294, 2025, 2, Downloaded from https://ceramics.onlinelibrary.wiley.com/doi/10.1111/ijag.16695 by Universitaet Bayreuth, Wiley Online Library on [18/03/2025]. See the Terms and Conditions (https://onlinelibrary.wiley.com/terms-and-conditions) on Wiley Online Library for rules of use; OA articles are governed by the applicable Creative Commons License

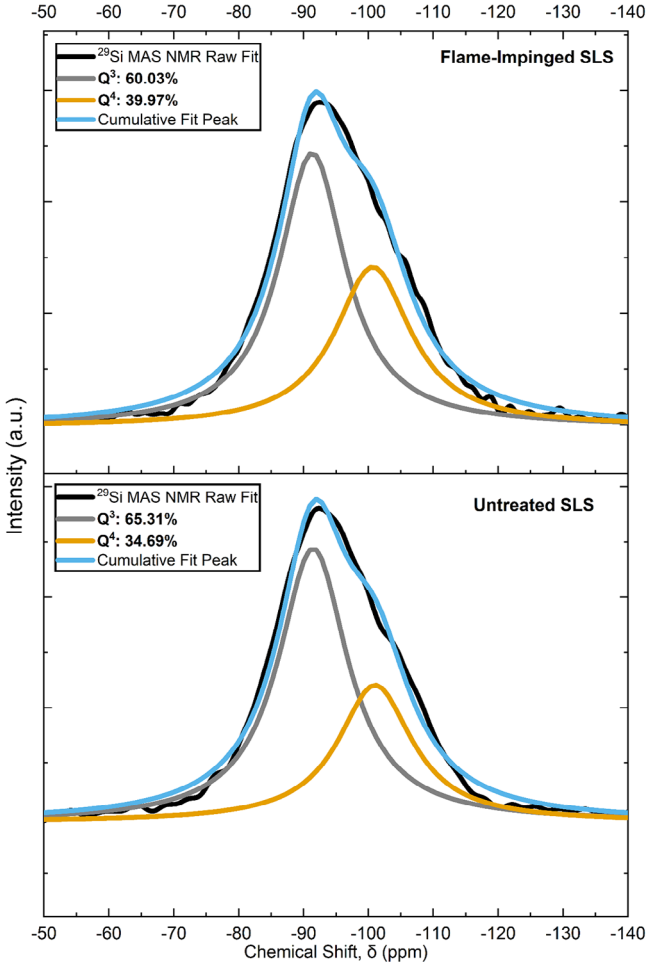

FIGURE 3 ^{29}Si MAS NMR spectral fits of untreated and flame-impinged SLS specimens for quantification of respective Q^n species by normalized integrated peak areas mentioned in the legends. R-square > .99 in both spectral fits. MAS NMR, magic angle spinning nuclear magnetic resonance.

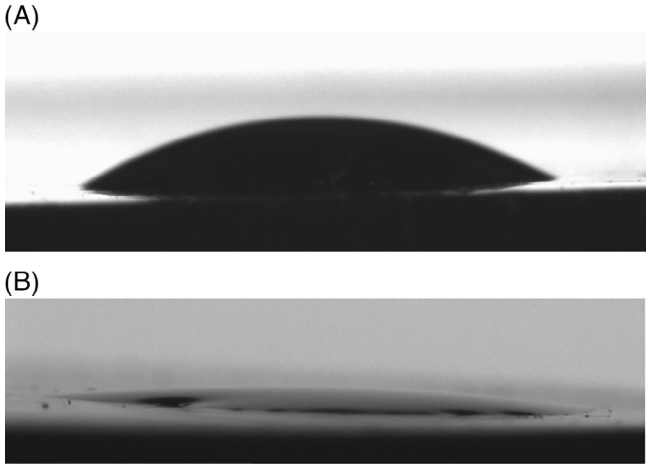

FIGURE 4 Static contact angle with respect to water (A) pristine SLS glass: 32° (B) flame-impinged SLS glass ≈ 0°—complete spreading—superhydrophilic surface. The volume of the water droplet is 2.5 μL. SLS, soda-lime-silica.

This reflects the absence of any effect of aging to deteriorate the property achieved. The interaction of the treated surface with the ambient atmosphere does not cause any significant alteration in surface chemistry to influence the contact angle. This is in contrast to the degradation of surface mechanical properties caused by ambient aging of a glass surface treated by superheated steam, as observed in our previous study.[26,28] The achievement of superhydrophilic SLS surface by high-temperature annealing at 900 K in a tube furnace that was reported in the past[20] was not an everlasting effect as the contact angle started to recover back again after 1 month. Our work stands out in the long-term stability of the superhydrophilic surface of as long as 3 years after the flame treatment of 10 s further highlighting the importance of the flame.

3 | CONCLUSION

In this study, the SLS glass surface was subjected to flame-impingement above its softening point for a brief interval of 10 seconds. The treatment altered the wetting characteristics of the surface, leading to superhydrophilicity. The subsurface structural modifications caused by the influence of flame-impingement were investigated to decipher the change in wetting behavior. X-ray photoelectron spectroscopic studies of the O1s spectral line revealed the increase in the concentration of BOs at the expense of hydrous species ($SiOH/H_2O$) in the near-surface region. This was indicative of silicate network repolymerization caused by the condensation of vicinal silanols to release molecular water. Thus, the network rearrangement in the subsurface region was associated with a notable increase in silicate network connectivity caused by the influence of flame impingement. The repolymerized BOs on the surface are proposed to act as absorption sites of water molecules to contribute to superhydrophilicity. Furthermore, solid-state ^{29}Si MAS NMR spectroscopy also corroborated the increase in silicate network connectivity in the bulk of the glass network with a conversion of Q^3 to Q^4 species by 5%. The AFM images substantiated the evidence of the conversion of open silicate rings into closed forms. The high surface energy of the repolymerized silicate network enhanced the chemical affinity of molecular water to promote extreme surface wettability—marked by the complete spread of a water droplet on a flame-impinged SLS surface. The property was discovered to be retained on exposure of the surface to aging in ambient atmosphere for 3 years. Thus, flame-impingement is a very promising way of achieving superhydrophilic SLS surfaces with everlasting effect.

20411294, 2025, 2, Downloaded from https://ceramics.onlinelibrary.wiley.com/doi/10.1111/ijag.16695 by Universitaet Bayreuth, Wiley Online Library on [18/03/2025]. See the Terms and Conditions (https://onlinelibrary.wiley.com/terms-and-conditions) on Wiley Online Library for rules of use; OA articles are governed by the applicable Creative Commons License

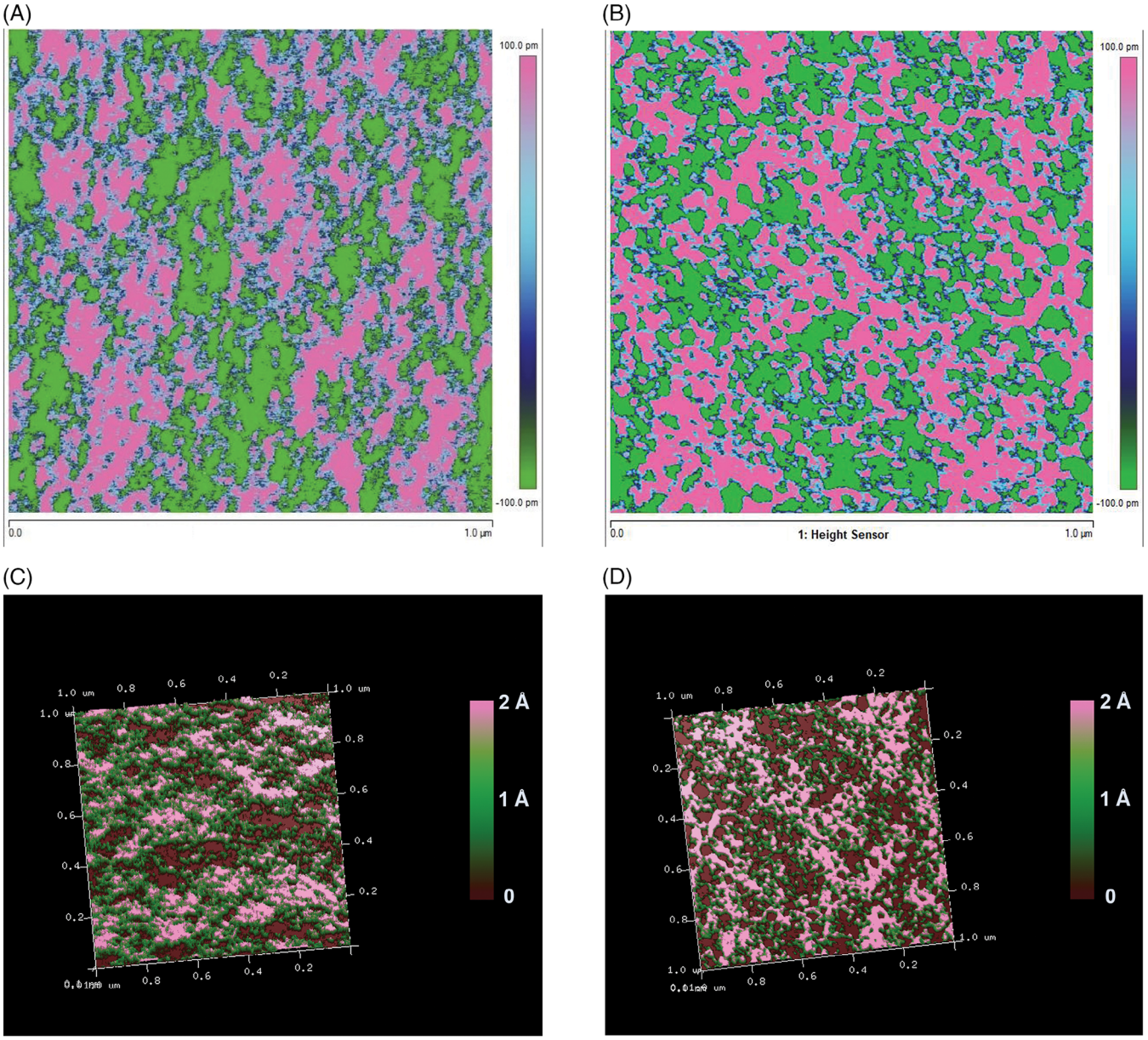

FIGURE 5 $1 \times 1\ \mu m^2$ AFM images scanned in tapping mode with z-resolution of 1 Angstrom (A) two-dimensional and (C) three-dimensional representation of pristine untreated SLS surface; (B) two-dimensional and (D) three-dimensional representation of flame-impinged SLS surface. The pristine surface is populated by open rings of silica tetrahedra (associated with nonbridging oxygens characterized by silanol groups), which are repolymerized into closed rings of diameters in the range of 30 to 80 nm, calculated by the ImageJ software. This is representative of the porosity on the glass surface on an atomic scale.[34] The *z*-scale corresponding to the height sensor in (A) and (B) ranges from a −100 picometer (voids within silicate rings marked by green) to a +100 picometer (pink). SLS, soda-lime-silica.

4 | METHODOLOGY

Soda-lime-silica container glass bottles with flat surfaces supplied by "Wiegand-Glas" were used in this study. The surfaces of the container bottles were not subjected to any hot-end or cold-end coatings during production. Glass samples with flat surfaces of diameter 25 mm and thickness 3 mm were drilled off the bottles (wet-cutting process), while ensuring the prevention of mechanical injury to the surface, except edges. The drilled cylindrical specimens were immersed in a static acetone bath for 15 min, rinsed in distilled water, followed by gently blow-drying by dry nitrogen gas (producer: "Riessner Gase"; purity: 99.999%, humidity≤ 5%) at room temperature—referred to as "pristine surface" before the flame-impingement process. The flame-impingement was carried out using the chemical energy of methane that was converted into thermal energy by a flame torch to reach surface temperatures

20411294, 2025, 2, Downloaded from https://ceramics.onlinelibrary.wiley.com/doi/10.1111/ijag.16695 by Universitaet Bayreuth, Wiley Online Library on [18/03/2025]. See the Terms and Conditions (https://onlinelibrary.wiley.com/terms-and-conditions) on Wiley Online Library for rules of use; OA articles are governed by the applicable Creative Commons License

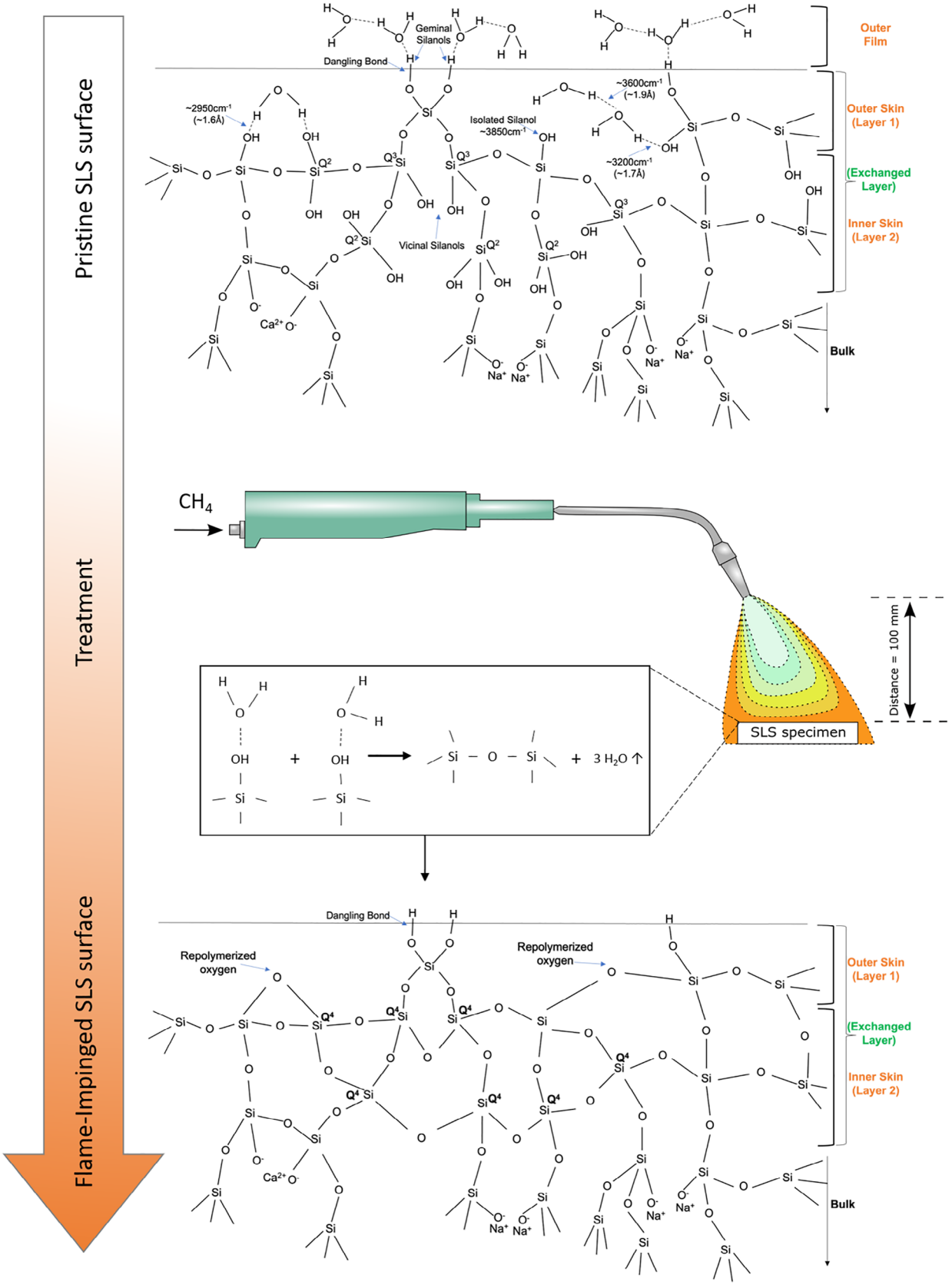

FIGURE 6 Schematic representation of the surface structures before and after flame-impingement indicating the repolymerized Q^4 units formed by the condensation of vicinal silanols, accompanied by loss of chemisorbed water. The highly reactive repolymerized bridging oxygens act as adsorption sites of water molecules to promote superhydrophilicity.

20411294, 2025, 2, Downloaded from https://ceramics.onlinelibrary.wiley.com/doi/10.1111/ijag.16695 by Universitaet Bayreuth, Wiley Online Library on [18/03/2025]. See the Terms and Conditions (https://onlinelibrary.wiley.com/terms-and-conditions) on Wiley Online Library for rules of use; OA articles are governed by the applicable Creative Commons License

above the softening point, as described in the text. The flame torch was at a distance of 100 mm from the glass surface for 10 s of treatment. The surface-sensitive characterization techniques, XPS and AFM were carried out immediately after the flame-impingement process to minimize the effect of the interaction of the surface with the ambient atmosphere, to the best possible extent. The elemental composition of the as-received glass, obtained by ICP-OES analysis consisted of (in wt%): 31.40% Si, 8.70% Na, 7.36% Ca, 1.14% Mg, .95% Al, .63% K, .26% Fe, and .03% Ti (rest mainly assigned to oxygen). It corresponds to the following oxide composition (in wt%): 71.4% SiO_2, 12.4% Na_2O, 10.9% CaO, 2% MgO, 1.9% Al_2O_3, .8% K_2O, .4% Fe_2O_3, and .1% TiO_2. The glass transition region (T_g) was determined to be confined within the range of 560–575°C, by dilatometric study (Netzsch 402 E/7/E-Py) at a heating rate of 5 K/min. The dilatometric softening point, T_d was 610°C.

The contact angle measurements were performed on the glass surface immediately after the flame-impingement using a drop shape analyzer Krüss DSA 100. A 2.5 μL water droplet was used for the measurement of static contact angle. The measurements were repeated after 1 and 3 years of the treatment to determine the long-term stability of superhydrophilicity caused by flame-impingement. The other analytical techniques are described in the following sections.

4.1 | X-ray photoelectron spectroscopy

XPS was performed by a PHI Versa Probe III spectrometer with an Al K alpha source (1486.6 eV). The target current on the specimen holder was 3 μA while the focus beam current at the Faraday cup was 302 nA. Surface charge neutralization was performed by a dual beam charge neutralization system that utilizes a cold cathode detector hood source and a very low energy ion source (<10 eV) to provide turnkey charge neutralization. The pass energy was 26 eV and the spectral resolution was about .2 eV. The samples were introduced to an ultra-high vacuum XPS chamber at a pressure on the order of 10^{-9} mbar.

Sequential XPS measurements were accompanied by argon ion sputtering (5 kV) at specific intervals and calibrated to depth scale using Ta_2O_5 as a standard reference. The necessary spectral fits (O1s and Si2p) were performed by MultiPak software using the Gaussian function after Shirley background correction[35]—to take into consideration the peak-broadening effect, which stems from the energy loss during inelastic scattering of electrons.

4.2 | Solid-state magic angle spinning nuclear magnetic resonance spectroscopy

Solid-state MAS ^{29}Si NMR spectroscopy of SLS glass powder (untreated, heat-treated, and steam-treated) was performed using Bruker Avance II 300 (magnetic field 7.05 T) in a 4-mm triple resonance probe. The samples were spun at 10.0 kHz. The spectra were obtained using a quantitative one-pulse experiment with a 90°-pulse length of 3.5 μs and a recycle delay of 60 s. ^{29}Si spectra were referenced indirectly with $N(SiMe_3)_3$/ σ(iso) = 2.4 ppm with respect to tetramethylsilane (σ(iso) = 0.0 ppm. Spectral fits were performed in an unconstrained manner by the Lorentzian deconvolution function to report the best fit in terms of the closest approach of R-square value to 1.

4.3 | Atomic force microscopy

High-resolution atomic force microscopy was performed by the "Bruker Dimension icon". A silicon nitride cantilever tip was used in tapping mode with a set point amplitude of 854 mV. A defined area of 1 × 1 μm^2 with 512 pixels was scanned on the pristine SLS surface. It was ensured that the same spot was scanned again after the process of flame-impingement, for a precise study of the alteration of surface topography.

ACKNOWLEDGMENTS

We gratefully acknowledge the financial support for the project 'VaporCoat' within the 'ForCycle II' research programme of the Bavarian State ministry of the Environment and Consumer Protection (grant BAF0150F-o74094). The access to the XPS/UPS facility (PHI 5000 VersaProbe III system) at the Device Engineering Keylab in the Bavarian Polymer Institute, University of Bayreuth is acknowledged; along with the fruitful experimental contributions of Felix Baier (Chair of Experimental Physics XI, University of Bayreuth). We appreciate the access to solid-state NMR experimental facilities granted by Nord Bayerisches NMR Zentrum (NBNC). The access to the AFM Keylab in the chair of Physical Chemistry II, University of Bayreuth is gratefully acknowledged.

Open access funding enabled and organized by Projekt DEAL.

ORCID

Barsheek Roy https://orcid.org/0000-0002-0197-8276
Anne Schmidt https://orcid.org/0000-0003-2556-8017
Andreas Rosin https://orcid.org/0000-0001-8835-5057

20411294, 2025, 2, Downloaded from https://ceramics.onlinelibrary.wiley.com/doi/10.1111/ijag.16695 by Universitaet Bayreuth, Wiley Online Library on [18/03/2025]. See the Terms and Conditions (https://onlinelibrary.wiley.com/terms-and-conditions) on Wiley Online Library for rules of use; OA articles are governed by the applicable Creative Commons License

REFERENCES

1. Griffith AA. VI. The phenomena of rupture and flow in solids. Philos Trans R Soc, A. 1921;221:163–98.
2. Varshneya AK. Stronger glass products: lessons learned and yet to be learned. Int J Appl Glass Sci. 2018;9:140–55.
3. Zhang Z, Kob W, Ispas S. First-principles study of the surface of silica and sodium silicate glasses. Phys Rev B. 2021;103:184201.
4. Cailleteau C, Angeli F, Devreux F, Gin S, Jestin J, Jollivet P, et al. Insight into silicate-glass corrosion mechanisms. Nat Mater. 2008;7:978–83.
5. Hellmann R, Cotte S, Cadel E, Malladi S, Karlsson LS, Lozano-Perez S, et al. Nanometre-scale evidence for interfacial dissolution-reprecipitation control of silicate glass corrosion. Nat Mater. 2015;14:307–11.
6. Gin S, Jollivet P, Fournier M, Angeli F, Frugier P, Charpentieret T, et al. Origin and consequences of silicate glass passivation by surface layers. Nat Commun. 2015;6:6360.
7. Deng L, Miyatani K, Suehara M, Amma S-I, Ono M, Urata S et al. Ion-exchange mechanisms and interfacial reaction kinetics during aqueous corrosion of sodium silicate glasses. npj Mater Degrad. 2021;5:15.
8. Macaulay JM. The polishing of surfaces. Nature. 1926;118:339.
9. Fauchais PL, Heberlein JVR, Boulos MI. Thermal Spray Fundamentals Ch. 5, US: Springer; 2014.
10. Tikkanen J, Eerola M, Rajala M. Coating glass by flame spraying. J Non-Cryst Solids. 1994;178:220–26.
11. Haller W, Deucker HC. Modification of glass surfaces by p-nitrobenzyl bromide. Nature. 1956;178:376–77.
12. Wei M, Bowman RS, Wilson JL, Morrow NR. Wetting properties and stability of silane-treated glass exposed to water, air and oil. J Colloid Interface Sci. 1993;157:154–59.
13. Park J, Lim H, Kim W, Ko JS. Design and fabrication of a superhydrophobic glass surface with micro-network of nano pillars. J Colloid Interface Sci. 2011;360:272–79.
14. Zhang L, Zhou AG, Sun BR, Shen KS, Yu HZ. Functional and versatile superhydrophobic coatings via stoichiometric silanization. Nat Commun. 2021;12:982–88.
15. Yu E, Kim SC, Lee HJ, Oh KH, Moon MW. Extreme wettability of nanostructured glass fabricated by non-lithographic, anisotropic etching. Sci Rep. 2015;5:9362–67.
16. Ye X, Cai D, Guo Y, Hou J. A facile method for producing superhydrophilic glasses via charge injection. AIP Adv. 2018;8:125225.
17. Yang L, Luo X, Chang W, Tian Y, Wang Z, Gao J, et al. Manufacturing of anti-fogging superhydrophilic microstructures on glass by nanosecond laser. J Manuf Processes. 2020;59:557–65.
18. Wang R, Hashimoto K, Fujishima A, Chikuni M, Kojima E, Kitamura A, et al. Light-induced amphiphilic surfaces. Nature. 1997;388:431–32.
19. Tettey KE, Dafinone MI, Lee D. Progress in superhydrophilic surface development. Materials Express. 2011;1:89–104.
20. Zhang D, Gao N, Yan W, Luo W, Zhang L, Zhao C, et al. Heat induced superhydrophilic glass surface. Mater Lett. 2018;223:1–4.
21. Nesbitt HW, Bancroft GM, Henderson GS, Ho R, Dalby KN, et al. Bridging, non-bridging and free (O^{2-}) oxygen in Na_2O-SiO_2 glasses: an X-ray photoelectron spectroscopic (XPS) and nuclear magnetic resonance (NMR) study. J Non-Cryst Solids. 2011;357:170–80.
22. Banerjee J, Bojan V, Pantano CG, Kim SH. Effect of heat treatment on the surface chemical structure of glass: oxygen speciation from in-situ XPS analysis. J Am Ceram Soc. 2017;101:644–56.
23. Simonsen ME, Sonderby C, Li Z, Sogaard EG. XPS and FT-IR investigations of silicate polymers. J Mater Sci. 2009;44:2079–88.
24. Roy B, Rosin A, Gerdes T, Schafföner S. Revealing the surface structural cause of scratch formation on soda-lime-silica glass. Sci Rep. 2022;12:2681.
25. Roy B, Baier F, Rosin A, Gerdes T, Schafföner S. Structural characterization of the near-surface region of soda-lime-silica by X-ray photoelectron spcectroscopy. Int J Appl Glass Sci. 2023;14:229–39.
26. Roy B, Rosin A, Gerdes T, Schafföner S. Transient subsurface hardening of soda-lime-silica glass by superheated steam. Glass Technol: Eur J Glass Sci Technol A. 2023;64(6):185–96.
27. Van der Heide P. X-ray photoelectron spectroscopy: an introduction to principles and practices. Hoboken: John Wiley & Sons, Inc. 2012.
28. Roy B. Surface modification of soda-lime-silica glass by superheated steam. Doctoral thesis. 2024. https://doi.org/10.15495/EPub_UBT_00007837
29. Solid-state NMR spectroscopy. Nat Rev Methods Primers. 2021;1:4.
30. Jones AR, Winter R, Greaves GN, Smith IH. MAS NMR study of soda-lime-silicate glasses with variable degree of polymerisation. J Non-Cryst. Solids. 2001;293–295:87–92.
31. DeRosa RL, Schader PA, Shelby JE. Hydrophilic nature of silicate glass surfaces as a function of exposure conditions. J Non-Cryst. Solids. 2003;331:32–40.
32. Drelich J, Chibowski E. Superhydrophilic and superwetting surfaces: definition and mechanisms of control. Langmuir. 2010;26:18621–23.
33. Ngo D, Liu H, Chen Z, Kaya H, Zimudzi TJ, Gin S, et al. Hydrogen bonding interactions of H2O and SiOH on a boroaluminosilicate glass corroded in aqueous solution. npj Mater. Degrad. 2020;4:1.
34. Sewell PA. Porous layers at glass surfaces. Nature. 1968;217:441–42.
35. Shirley DA. High-resolution X-ray photoemission spectrum of the valence bands of gold. Phys Rev B. 1972;5:4709–14.

SUPPORTING INFORMATION

Additional supporting information can be found online in the Supporting Information section at the end of this article.

How to cite this article: Roy B, Schmidt A, Rosin A, Gerdes T. Flame-impingement-induced superhydrophilicity of soda-lime-silica glass surface. Int J Appl Glass Sci. 2025;16:e16695. https://doi.org/10.1111/ijag.16695

20411294, 2025, 2, Downloaded from https://ceramics.onlinelibrary.wiley.com/doi/10.1111/ijag.16695 by Universitaet Bayreuth, Wiley Online Library on [18/03/2025]. See the Terms and Conditions (https://onlinelibrary.wiley.com/terms-and-conditions) on Wiley Online Library for rules of use; OA articles are governed by the applicable Creative Commons License